Colloid Polym Sci (2006) 284: 1131–1138
DOI 10.1007/s00396-006-1490-y

ORIGINAL CONTRIBUTION

Amornrat Viriyaroj
Hiroshi Kashiwagi
Masaharu Ueno

Solubilization of egg phosphatidylcholine liposomes by sodium taurocholate: partition behavior and morphology

Received: 8 August 2005
Accepted: 9 January 2006
Published online: 4 May 2006

A. Viriyaroj ·
H. Kashiwagi · M. Ueno (✉)
Faculty of Pharmaceutical Sciences,
University of Toyama,
2630 Sugitani,
Toyama, 930-0194, Japan
e-mail: mueno@pha.u-toyama.ac.jp
Tel.: +81-76-4347565
Fax: +81-76-4345050

Abstract Solubilization process of egg yolk phosphatidylcholine (EggPC) liposomes by sodium taurocholate (TC) was performed using membrane dialysis technique. Turbidity, apparent particle size, Cl^- permeability, membrane fluidity measured by electron spin resonance spectroscopy (ESR), and structural changes observed by freeze-fracture electron microscopy were investigated. The concentrations of TC were analyzed by high-performance liquid chromatography to determine the incorporation of TC in membrane phase and apparent partition coefficient. When TC concentration in water phase (D_w) was lower than 1.41 mM, or effective ratio of TC to EggPC (R_e) was less then 0.14, the partition coefficient was independent of the TC concentration and was 90 M^{-1}, where the membrane permeability of Cl^- was rather small. Upon increasing the concentrations in the range of 1.41 mM$\leq D_w<$3.10 mM ($0.14\leq R_e<0.21$), the apparent partition coefficient decreased and membrane permeability markedly increased.
The coexistence of small vesicles and bilayer fragments were observed in this region. At 3.10 mM$\leq D_w<$ 3.53 mM ($0.21\leq R_e<0.59$), the steep decrease in turbidity was accompanied with the gradual increase in apparent partition coefficient, suggesting the formation of mixed micelles. The freeze-fracture electron micrographs confirmed the transformation of saturated bilayers to wormlike mixed micelles. When a further increase in TC ($D_w\geq 3.53$ or $R_e\geq 0.59$) was applied, the turbidity and apparent particle sizes became small. Transformation of the wormlike structure to ellipsoid mixed micelles was observed. The ESR spectra showed that TC/EggPC mixed micelles still retain a somewhat orderly structure.

Keywords Solubilization · Liposomes · Phosphatidylcholine · Electron microscopy

Introduction

The membrane solubilization by detergent is known as the reverse of the reconstitution after removal of detergent from lipid/detergent mixed micelles. Liposomes have been used as models of biological membranes to form protein reconstitution or to mimic membrane barriers providing the functional proteoliposomes [1]. The study on the solubilization of phospholipids provides an understanding of the available information for an application in reconstitution. For this reason, the mechanism of vesicle–micelle transition has been extensively investigated in the past decades [2–6]. Generally, the solubilization of liposomes by a detergent was described as detergent partitions into vesicle membranes without significant alteration in membrane structure at low concentration. Above certain effective ratio of detergent to lipid, the barrier efficiencies of vesicle membrane diminish. With an increase in detergent con-

centration, bilayers become saturated with detergent. A further increase in detergent concentration leads to complete solubilization [7, 8].

Bile salts are physiological detergents, which have a hydrophobic backbone with one to three hydroxyl groups. Their solubilizing properties are extensively useful in several fundamental and biochemical process. They have been used for the development of an effective solubilization–reconstitution protocol because they can readily solubilize the protein from the membrane without or with little initiating denaturation [9, 10]. Additionally, information of interaction between lipid and bile salt leads to the understanding of the physiological function of bile in emulsifying fatty materials in the gastrointestinal tract [11]. Among bile salts, sodium cholate is most commonly used to study the vesicle destruction mechanism. The effect of sodium cholate on liposomes has been studied by a number of techniques such as nuclear magnetic resonance, electron spin resonance (ESR), differential scanning calorimetry, quasi elastic and static light scattering, cryo-transmission electron microscopy (TEM), and freeze-fracture electron microscopy [2, 6, 12–17]. Due to the similar properties to sodium cholate in biocompatibility, charge, and critical micelle concentration value, sodium taurocholate (TC) is an alternative detergent used in biochemistry research [18]. However, little has been published about the interaction of sodium taurocholate on liposomes.

The previous studies in our laboratory on the solubilization of liposomes by sodium cholate have shown that the small vesicles containing large amounts of detergents were not easily fusible in contrast to the case of octylglucoside as a detergent. For the vesicle formation upon sodium cholate removal from sodium cholate/phospholipid mixed micelles, it was found that small vesicles were formed by dialysis or by dilution. However, in the presence of 5 mM Ca^{2+}, large vesicles were produced by dialysis, while small vesicles were obtained by dilution. These suggested that the size regulation of vesicles related to an electrostatic repulsion of the surface of vesicles and rate of detergent removal [15, 19].

In the current study, we reported the changes in physicochemical properties in the solubilization process of liposomes by sodium taurocholate. The partition behavior of sodium taurocholate between the membrane and water phases was clarified. The results obtained will provide useful information in the kinetic aspect on the interaction of sodium taurocholate on liposomes.

Materials and methods

Materials

Egg yolk phosphatidylcholine (EggPC, COATSOME NC-50; purity more than 95%) was purchased from NOF (Tokyo, Japan). Sodium taurocholate (minimum 95%) was provided from Sigma (USA). 5-Doxylstearic acid (5-DS) was obtained from Aldrich (USA). Methanol [high-performance liquid chromatography (HPLC) grade], potassium dihydrogen phosphate, and *N*-Tris(hydroxymethyl)methyl-2-aminoethanesulfonic acid (TES) were purchased from Nacalai Tesque (Kyoto, Japan). Sephadex G-75 was supplied by Pharmacia Biotech (Sweden). Phosphoric acid and dialysis membrane molecular weight cutoff 14,000 were provided from Wako Pure Chemicals (Tokyo, Japan). All other chemicals were of analytical grade from Nacalai Tesque. All buffers were filtered before use to minimize interference from any extraneous particulate matter.

Liposome preparation

EggPC liposomes were prepared by extrusion method. A known amount of EggPC was dissolved in chloroform/methanol (2:1, v/v). The lipid was deposited as a thin film on test tube under a stream of nitrogen gas. The lipid film was then placed under vacuum overnight to remove the remaining organic solvent. The lipid film was hydrated with an appropriate volume of TES buffer (20 mM TES and 150 mM NaCl, pH 7.0) to produce multilamellar vesicles (MLV). The MLV was frozen (liquid nitrogen, −196 °C) and thawed (water bath, 40 °C) five times, then each was extruded ten times under nitrogen pressure through double-stacked polycarbonate membrane filters (Nucleopore, Costar, USA) with decreasing pore size of 0.6 and 0.2 μm, yielding extruded liposomes. After the preparation, the actual phospholipid concentration was determined as total phosphate based on the method of Ames [20]. Thereafter, liposomes were diluted to a concentration of 10 mM with TES buffer and used as stocked suspension within 7 days after preparation. Liposomes were purged with argon gas and kept at 4 °C to avoid lipid degradation.

The extruded liposomes were incubated with sodium taurocholate solution in a shaking water bath at 25 °C for 1 day by equilibrium dialysis cell, separated by a dialysis membrane. The membrane was kept in TES buffer before use [8].

TC analysis and apparent partition coefficient

The HPLC condition used in TC analysis was adapted from the method of Rossi et al. [21]. The samples were adjusted to an appropriate concentration of 0.15–5 mM by addition of purified water. A 30-μl sample was injected to a C-18 reverse phase column (Inersil ODS 5 μm, column dimension 25 cm × 4.6 mm, GL Sciences, Japan) connected to a HPLC apparatus (Water LC Module I^{plus}, Waters, USA). The mobile phase was methanol (0.01 M phosphate buffer 78:22). A volume of 4.2 ml of 5 M NaOH per liter of

solvent was added to the mixture; thereafter, the pH of the system was adjusted to about 5.4 by addition of 85% phosphoric acid. The flow rate was 1.35 ml/min and produced pressure was 15.5–15.7 MPa. The UV detector was set at 205 nm. The retention time of TC was 6.5–6.7 min.

The effective ratio of TC to EggPC (R_e) can be calculated according to

$$R_e = D_B/L \tag{1}$$

where D_B is the concentration of TC in the membrane phase. L is the concentration of EggPC.

Partition coefficient (K) can be defined by Eq. 2.

$$K = X/D_W = D_B/(L + D_B)D_W \tag{2}$$

where X is the mole fraction of the detergent in the membrane phase. D_W is the concentration of the detergent in equilibrium in the water phase.

Size and turbidity measurements

The mean particle sizes of the aggregates of sodium taurocholate/EggPC system were measured using dynamic light scattering (ELS-6000, Photal Otsuka Electronics, Osaka, Japan). Turbidity of EggPC suspension was obtained with a 0.25-cm wide cuvette at 500 nm using a UV spectrophotometer (UV-160, Shimadzu, Japan). All samples were determined without any dilution.

Chloride permeation

Cl^- permeability was determined according to the procedure previously described [8] with the following slight modification. An ion-selective electrode meter (Model 920 A, Orion Research, USA), connected to a Cl^- selective electrode (Model 9417B, Thermo Orion, USA), was used to measure the efflux of Cl^- into the $NaNO_3$ solution. The entrapped Cl^- was separated from untrapped Cl^- by Sephadex G-75 gel (1×15 cm column). The eluent was 20 mM TES/150 mM $NaNO_3$ buffer with equilibrium concentration of TC in mixed TC vesicles (pH 7.0). If Cl^- permeation obeys first-order kinetics, Eq. 3 is obtained.

$$\ln(C_\infty - C_t) = \ln(C_\infty - C_0) - kt \tag{3}$$

where k is the rate constant for permeation of Cl^-. C_t is the measured Cl^- concentration (in millimolar) at time t, C_0 is the initial Cl^- concentration, and C_∞ is the Cl^- concentration after complete liberation of entrapped Cl^- attained by adding 20% Tritron X-100. k is the slope of the line obtained by plotting $\ln(C_\infty - C_t)$ against t.

The permeability coefficient (p) for Cl^- was obtained from the relation

$$p/k = (\textit{internal volume/vesicle})/(\textit{membrane area/vesicle}) \tag{4}$$

ESR spectroscopy

The mixed TC aggregates were added to a test tube containing a thin film of spin probe (5-DS) at a molar ratio of 1:100. The sample was packed in the tip of capillary tube (20 μl) after it was swirled and equilibrated for at least 2 h. Measurement was carried out with an X-band spectrometer (100 kHz modulation, JES-TE100, JEOL, Japan) equipped with temperature control accessory. The condition was set as follows: microwave power, 12 mW; amplitude, 79; time constant, 0.1 s; scan field, ±5 mT; scanning time, 4 min. The peaks of external manganese dioxide were used for the determination of peak position and amplitude of the spin probe. The order parameter, S, of 5-DS was calculated using Gaffney's equation [22]

$$S = \frac{T_\parallel - (T_\perp + C)}{T_\parallel - 2(T_\perp + C)}$$
$$C = 0.14 - 0.0053(T_\parallel - T_\perp) \tag{5}$$

where $T_\parallel$ and $T_\perp$ are outer hyperfine splitting and inner hyperfine splitting, respectively.

Freeze-fracture electron microscopy

Small aliquot of dispersion was dropped on specimen holder and rapidly frozen into liquid nitrogen. The sample was then fractured under vacuum at −120 °C in a FR-7000B apparatus (Hitachi, Japan). Shadowing of fractured face with platinum/carbon followed by carbon was performed at an angle of 45° and 90° for each coating, respectively. The replica was cleaned with a solution of commercial bleach and purified water. The clean replica was examined using a transmission electron microscope (JEM-200CX, JEOL, Japan).

Results

Partition behavior of TC between the membrane phase and water phase

Figure 1 represents the partition behavior of TC in the membrane and water phases. The ordinate represents TC concentration in mole fraction in the membrane phase, and the abscissa represents TC concentration in the water phase. The slope of this plot represents the apparent partition coefficient. When the concentration of TC in water phase (D_w) was lower than 1.41 mM or an effective ratio less than 0.14, this plot displayed a linear relation. The partition coefficient obtained from the slope was 90 M^{-1}. In 1.41 mM≤D_w<3.10 mM (point A–B), the slope became lower. The calculation from each point of X and D_w found that the partition coefficient decreased to 56 M^{-1}. In this region, the turbidity gradually decreased (Fig. 2). When 3.10 mM≤D_w<3.53 mM (point B–C), the apparent partition coefficient gradually increased.

Change in turbidity and apparent particle size

The change in turbidity at 500 nm upon incorporation of TC is plotted against an effective ratio (R_e), as depicted in Fig. 2. When small concentration of TC was added to liposomes, the turbidity first decreased until R_e=0.03, followed by a more or less constant value. Then a further increase in TC led to a slight increase in turbidity during 0.14≤R_e≤0.16. Above R_e of 0.16, the turbidity drastically decreased. The turbidity was nearly 0 when R_e≥0.59.

The change in apparent particle size of EggPC liposomes as a function of R_e is shown in Fig. 3. The mean diameter of TC-free vesicles was 177 nm and the concentration of phospholipid was kept at about 10 mM. Similar to the turbidity pattern, the first decrease in particle size was also observed. In R_e 0.01–0.11, the mean diameters of TC-containing liposomes are smaller than initial extruded vesicles of about 160 nm. Subsequently, a slight increase in apparent particle size was observed when R_e exceeded 0.11. Above R_e of 0.37, the apparent particle size became decreased again. With further increase in TC concentration (R_e≥0.59), the apparent particle sizes were very small, supporting the formation of mixed micelles.

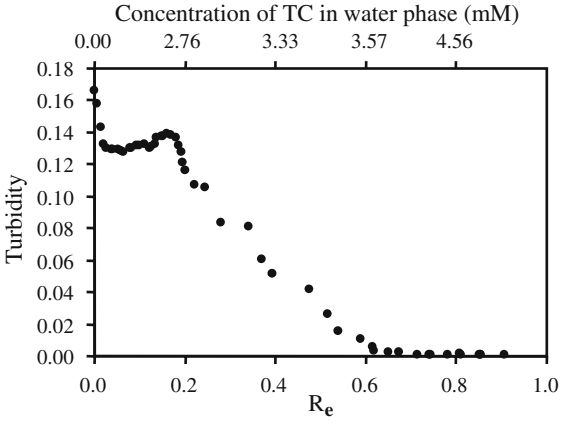

Fig. 2 Change in optical density of extruded liposomes on the effective ratio of TC to EggPC (R_e). The optical density was measured at 500 nm against TES buffer (pH 7) at 25 °C

Membrane barrier efficient

The effect of TC concentration on membrane permeability coefficient is shown in Fig. 4. The permeability coefficient (p) of TC-free vesicles was about 6.78×10^{-11} cm/s, corresponding to the Cl^- efflux rate constant (k) of 2.7×10^{-5} s^{-1}. The slight increase in Cl^- permeability with the incorporation of TC up to R_e of 0.15 was observed. The steep increase in membrane permeability at R_e of 0.17 suggests that the barrier efficiency of the membrane diminished.

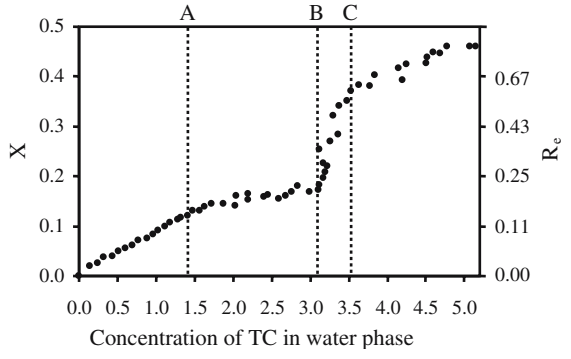

Fig. 1 Partition equilibrium of TC between the membrane phase and water phase at 25 °C. Points *A*, *B*, and *C* represent the effective ratio of of TC to EggPC (R_e) at 0.14, 0.21, and 0.59, respectively

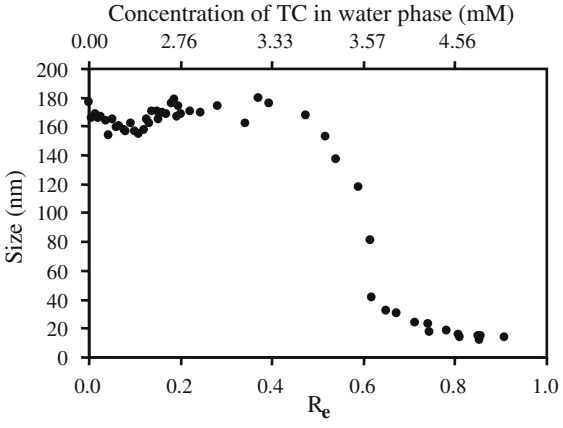

Fig. 3 Change in apparent particle size of extruded liposomes on the effective ratios of TC to EggPC (R_e) at 25 °C

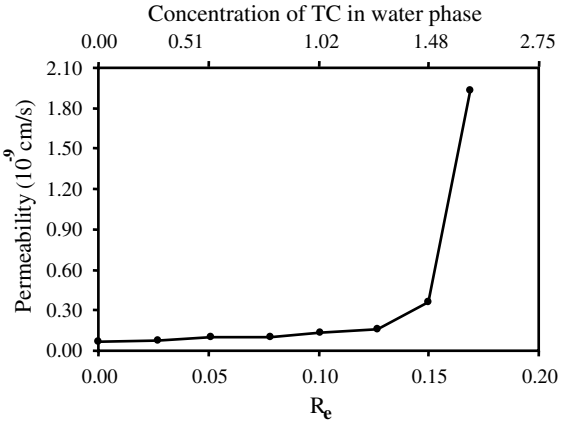

Fig. 4 Dependences of permeability coefficient of entrapped Cl^- through vesicle membrane on the effective ratio of TC to EggPC (R_e) at 25 °C

Figure 5 represents plots of the partition coefficient and permeability coefficient against R_e. An abrupt rise in membrane permeability was found to be accompanied with a lowering of the partition coefficient.

Membrane state and order parameter

The ESR spectra of 5-DS in TES buffer and TC-free or TC-containing liposomes at different R_e are shown in Fig. 6. A 5-DS in TES buffer can rotate freely and then the sharp triplet bands of isotropic spectrum was obtained (Fig. 6a). On the contrary, the ESR spectrum of 5-DS in PC liposomes represents anisotropy, indicating the restriction in mobility of the spin probe inside the EggPC bilayers (Fig. 6b). The outermost separation of high-field hyperfine splitting decreased with the addition of TC into liposomes, leading to the decrease in order parameter as depicted in Fig. 6f. The incorporation of TC into extruded liposomes resulted in the change of order parameters as illustrated in Fig. 7. The order parameters slightly decreased with an addition of TC concentration less than R_e of 0.21; however, the decrease was small and simple. At $R_e \geq 0.21$, the order parameter markedly decreased, suggesting the beginning of vesicle solubilization.

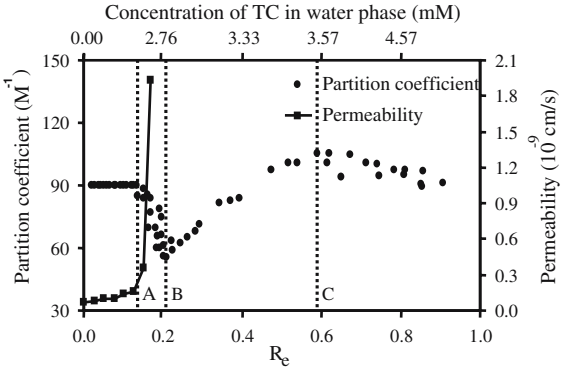

Fig. 5 Plots of partition coefficient of TC (●) and permeability coefficient (■) as a function of the effective ratio of TC to EggPC (R_e) at 25 °C

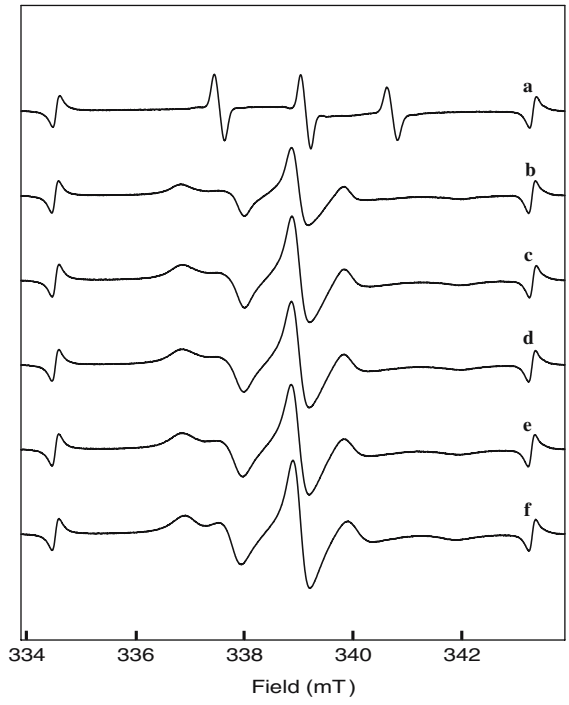

Fig. 6 ESR spectra of 5-DS in **a** TES buffer, **b** TC-free EggPC liposomes, TC-containing liposomes at R_e of **c** 0.10, **d** 0.19, **e** 0.34, and **f** 0.65, respectively, at 25 °C

Freeze-fracture transmission electron microscopy

Morphology of the TC–EggPC mixed aggregates were investigated by freeze-fracture transmission electron mi-

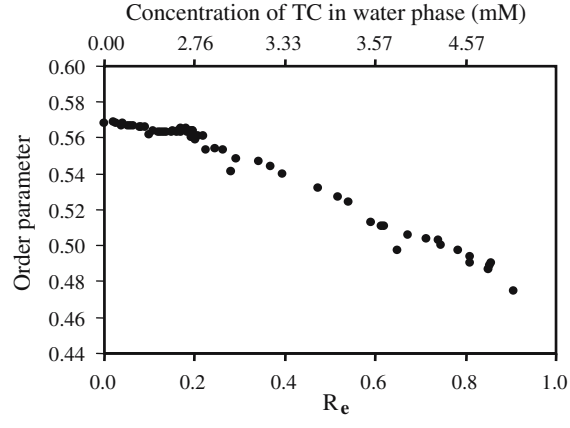

Fig. 7 Dependences of order parameter of 5-DS of TC-containing EggPC liposomes on the effective ratio (R_e) during solubilization process at 25 °C

croscopy as illustrated in Fig. 8. In the absence of TC (R_e=0) and at low concentration of TC (R_e=0.05), spherical vesicles were mainly observed (Fig. 8a,b). At R_e of 0.07 and 0.10, distorted vesicles were seen in coexistence with spherical vesicles (Fig. 8c,d). Increasing TC concentration up to R_e of 0.19 led to the disruption of liposomes resulting in the coexistence of rather small vesicles and bilayer fragments (Fig. 8e,f). At R_e of 0.20, most of bilayer fragments became smaller and small size vesicles were still observed (Fig. 8g). Upon increasing the TC concentration up to R_e of 0.24, the fraction of bilayer fragments became smaller and thinner as shown in Fig. 8h. Further addition of TC led to the formation of wormlike structures or flexible micelles as illustrated in Fig. 8i,j. At higher TC concentration, the lengths of the rod micelles became shorter and the ellipsoid mixed micelles was observed (Fig. 8k). With further increase in TC up to R_e of 0.65, the ellipsoid micelles became dominant (Fig. 8l).

Discussion

Dialysis technique was adopted to avoid possible solubilization by direct addition of a detergent in the micellar state and to obtain monomer concentration of the detergent in equilibrium between vesicle and buffer solution. The effective ratio of detergent to phospholipids (R_e) was used to determine the changes of membrane properties during transformation of the liposomes to mixed micelles. The overall solubilization process of EggPC liposomes by TC revealed that no notable increase in turbidity and apparent particle size were observed. This agrees with the previous data when sodium cholate was used as surfactant [15]. On the other hand, notable increase in turbidity and apparent particle size were found during solubilization process in the case of octylglucoside or CHAPS [23, 24]. This difference can be explained by the consideration that anionic charge at head group of surfactant (TC or sodium cholate) could prevent the fusion of vesicles containing large amount of surfactant, SUV* (see references 19, 24), during solubilization process.

At very small addition of TC, the gradual decrease in turbidity corresponding to a slight decrease in apparent particle size can be observed (Figs. 2 and 3). These results are in accordance with other reports, in that the slight decrease in optical density from the initial vesicles over a small increase in TC concentration to liposomes by direct addition method [25]. These observations indicate that the initial decrease in turbidity is independent of method of TC addition to liposomes. Furthermore, the first progressive

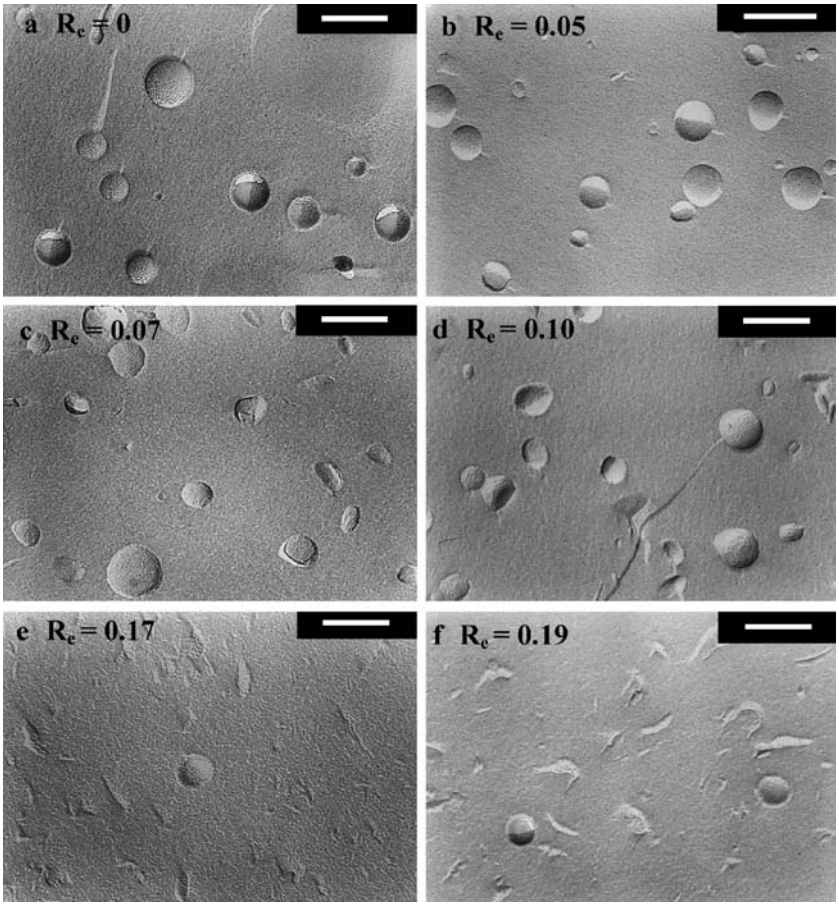

Fig. 8 Freeze-fracture electron micrographs of TC-containing EggPC liposomes at the effective ratio (R_e) of **a** 0, **b** 0.05, **c** 0.07, **d** 0.10, **e** 0.17, **f** 0.19. *Bar* represents 200 nm. Freeze-fracture electron micrographs of TC-containing EggPC liposomes at the effective ratio (R_e) of **g** 0.20, **h** 0.24, **i** 0.34, **j** 0.37, **k** 0.47, and **l** 0.65. *Bar* represents 200 nm

Fig. 8 (continued)

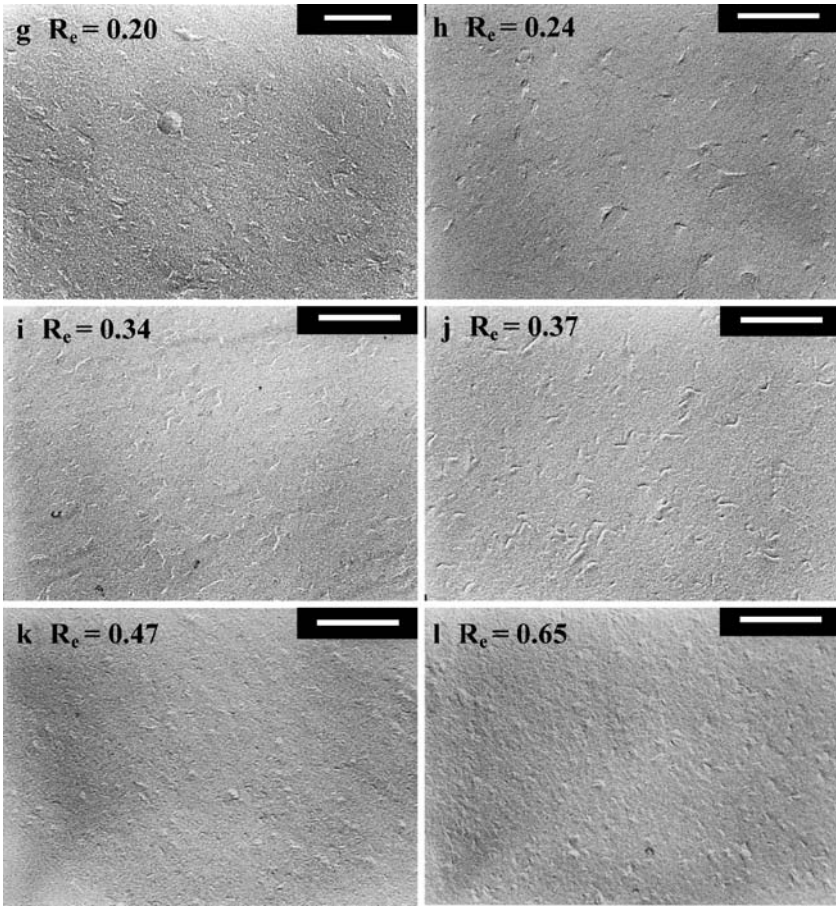

decrease in turbidity after small addition of other anionic surfactants was also reported [7, 27]. However, these observations have not been found when octylglucoside was added to liposomes under similar conditions [24]. The contraction of mixed vesicles is a possible explanation when low concentrations of TC were incorporate into vesicles. Increasing TC up to R_e of 0.07 and 0.10 resulted in ellipsoid and distorted vesicles (Fig. 8c,d). When the concentration of TC was lower than 1.41 mM in the water phase, TC partitioned to membrane with a constant partition coefficient value without significant destruction of vesicles (Fig. 8a–d). Our results of the partition of TC to EggPC liposomes at low concentration of TC differed from those of Andrieux et al. [26]. They reported that no insertion of TC was observed in the first stage of the solubilization process. One possible explanation regarding this discrepancy is the different experimental method. They determined in situ the partition coefficient of TC between the aggregates and the aqueous medium upon continuous addition of TC into liposomes with fast rate. On the other hand, the addition of TC into liposomes in our experiments was performed by using dialysis membrane. The partition behavior was pursued after 24 h of incubation. Therefore, the data in our experiments were obtained at equilibrium systems and at lower concentration of TC than those of Andrieux et al.

Upon increasing TC in the range of 1.41 mM$\leq D_w$<3.10 mM, the apparent partition coefficient decreased (Fig. 1). This result is in accordance with partition behavior of sodium cholate/EggPC system and octylglucoside/EggPC system in our previous works [13, 23]. The dramatic increase in membrane permeability at R_e of 0.17 suggests that the more addition of TC in vesicle membranes lead to an increase in the formation of transient structure. Freeze-fracture electron micrographs clearly showed the coexistence of the vesicles and bilayer fragments, whereas the small degree in reduction of order parameter in this range was obtained (Fig. 7). These indicate that the restriction of mobility of 5-DS surrounded by EggPC molecules in bilayer fragments was similar to that in vesicles. The decrease in apparent partition coefficient can be explained by two possible reasons—the establishment of electrostatic potential on vesicle surface by the negative charge of TC and/or the formation of small mixed vesicles accompanied with the bilayer fragments. In this region, only small vesicles were observed (Fig. 8e,f). The abrupt decrease in Cl^- supported the data from freeze-fracture micrographs.

During 3.10 mM$\leq D_w$<3.53 mM (0.21$\leq R_e$<0.59), the partition coefficient increased with an increase in TC

concentration. This indicates that the addition of TC up to this range brings about the increase in TC in the membrane phase. The transformation of vesicles to mixed micelles is responsible in ascribing the increase in apparent partition coefficient, as can be seen in Figs. 8h and 9k. The obvious decrease in order parameter of 5-DS in this region indicates that solubilization occurred (Fig. 7). The interesting feature of Fig. 6 is that the ESR spectra of 5-DS of TC/EggPC system in micellar state (Fig. 6f) still remain to be anisotropic in contrast with those of the octylglucoside/EPC system [24]. This suggests that the motion of spin probe is restricted even in the micellar state. The saturation of TC in bilayers progressively transformed to mixed micelles. The effective ratio at the beginning of solubilization process ($R_e$sat) and the minimum effective ratio for complete solubilization ($R_e$sol) were 0.21 and 0.59, respectively.

The structures of bile salt–phospholipid mixed micelles are still a controversial issue. In early studies, the basic structure of bile salt–phospholipid system as a disk model was proposed by Small [28] and Mazer et al. [29]. However, the data obtained by small-angle neutron scattering and size exclusion HPLC have suggested that the general feature of bile salt/phospholipids mixed micelles was consistent to rodlike mixed micelles [30, 31]. The experiment, based on cryo-TEM, described the flexible cylindrical structures in these systems [16]. Additionally, the hollow cylindrical model was characterized as the aggregate structure performed by the static laser light scattering and electrophoretic light scattering in sodium cholate/EggPC system [13]. Recently, Egelhaaf and Schurtenberger [32] and Cohen et al. [14] proposed the structure of wormlike mixed micelles in bile salt/EggPC system determined by static light scattering and dynamic light scattering. Our data, based on freeze-fracture electron micrographs, allowed us to support the wormlike mixed micelles model in TC/EggPC system because they were mainly observed in the region of $3.10 \leq D_w < 3.53$ (Figs. 8i–k).

Further increase in TC concentration ($D_w \geq 3.53$) led to a very low turbidity and small apparent particle size, suggesting structural arrangement to mixed micelles. Freeze-fracture electron micrograph confirmed the formation of prolate ellipsoid mixed micelles (Fig. 8l).

In summary, the vesicle–micelle transition of EggPC liposomes by TC is described by, at least, four-stage model. In the first stage, TC partitions to lipid bilayers resulting in mixed bilayer vesicles without significant destruction of lipid bilayers. In the second stage, the small mixed vesicles coexisted with bilayer fragments. In this stage, the decrease in partition coefficient was observed. In the third stage, the bilayers transformed into wormlike mixed micelles. In the fourth stage, the solubilization of liposome into mixed micelles was completed. The wormlike mixed micelles progressively rearranged to ellipsoid mixed micelles.

References

1. Levy D, Gulik A, Seigneuret M, Rigaud JL (1990) Biochemistry 29:9480–9488
2. Paternostre MT, Roux M, Rigaud JL (1988) Biochemistry 27:2668–2677
3. Almog S, Litman BJ, Wimley W, Cohen J, Wachtel EJ, Barenholz Y, Ben-Shaul A, Lichtenberg D (1990) Biochemistry 29:4582–4592
4. Lasch J, Hoffmann J, Omelyanenko WG, Klibanov AA, Torchilin VP, Binder H, Gawrisch K (1990) Biochim Biophys Acta 1022:171–180
5. Schnitzer E, Lichtenberg D, Kozlov MM (2003) Chem Phys Lipids 126:55–76
6. Bayerl TM, Werner GD, Sackmann E (1989) Biochim Biophys Acta 984:214–224
7. Silvander M, Karlsson G, Edwards K (1996) J Colloid Interface Sci 179: 104–113
8. Ueno M (1987) Biochim Biophys Acta 904:140–144
9. Jones MN (1999) Int J Pharm 177: 137–159
10. Silvius JR (1992) Annu Rev Biophys Biomol Struct 21:323–348
11. Moschetta A, Frederik PM, Portincasa P, vanBerge-Henegouwen GP, van Erpecum KJ (2002) J Lipid Res 43:1046–1053
12. Sun C, Kashiwagi H, Ueno M (2002) Chem Pharm Bull (Tokyo) 50: 1145–1150
13. Sun C, Sano Y, Kashiwaki H, Ueno M (2002) Colloid Polym Sci 280: 900–907
14. Cohen DE, Thurston GM, Chamberlin RA, Benedek GB, Carey MC (1998) Biochemistry 37:14798–14814
15. Sun C, Ueno M (2000) Colloid Polym Sci 278:855–863
16. Walter A, Vinson PK, Kaplun A, Talmon Y (1991) Biophys J 60: 1315–1325
17. Almog S, Kushnir T, Nir S, Lichtenberg L (1986) Biochemistry 25:2597–2605
18. Naito M, Tsuruo T (1995) J Cancer Res Clin Oncol 121:582–586
19. Ueno M, Kashiwagi H, Hirota N (1997) Chem Lett 217–218
20. Ames BN (1966) Methods Enzymol 8:115–117
21. Rossi SS, Converse JL, Hofmann AF (1987) J Lipid Res 28:589–595
22. Sefton BM, Gaffney BJ (1974) J Mol Biol 90:343–358
23. Ueno M (1989) Biochemistry 28: 5631–5634
24. Ueno M, Hirota N, Kashiwagi H, Sagasaki S (2003) Colloid Polym Sci 282:69–75
25. Ramaldes GA, Fatttal E, Puisieux FOM (1996) Colloids Surf B Biointerfaces 6:363–371
26. Andrieux K, Forte L, Lesieur S, Paternostre M, Ollivon M, C Grabielle-Madelmont C (2004) Pharm Res 21:1505–1516
27. Lopez O, Cocera M, Wehrli E, Parra JL, de la Maza A (1999) Arch Biochem Biophys 367:153–160
28. Small DM (1967) Gastroenterology 52:607–610
29. Mazer NA, Benedek GB, Carey MC (1980) Biochemistry 19:601–615
30. Nichols JW, Ozarowski J (1990) Biochemistry 29:4600–4606
31. Hjelm RP, Thiyagarajan P, Alkan-Onyuksel H (1992) J Phys Chem 96:8653–8661
32. Egelhaaf SU, Schurtenberger P Shape (1994) J Phys Chem 98:8560–8573